(2)

AD

TECHNICAL REPORT ARCCB-TR-88011

ELASTIC, STRENGTH, AND STRESS RELAXATION PROPERTIES OF A723 STEEL AND 38644 TITANIUM FOR PRESSURE VESSEL APPLICATIONS

J. H. UNDERWOOD

R. R. FUJCZAK

R. G. HASENBEIN

MARCH 1988

US ARMY ARMAMENT RESEARCH,
DEVELOPMENT AND ENGINEERING CENTER
CLOSE COMBAT ARMAMENTS CENTER
BENÉT LABORATORIES
WATERVLIET, N.Y. 12189-4050

DISCLAIMER

The findings in this report are not to be construed as an official Department of the Army position unless so designated by other authorized documents.

The use of trade name(s) and/or manufacturer(s) does not constitute an official indorsement or approval.

DESTRUCTION NOTICE

For classified documents, follow the procedures in DoD 5200.22-M, Industrial Security Manual, Section II-19 or DoD 5200.1-R, Information Security Program Regulation, Chapter IX.

For unclassified, limited documents, destroy by any method that will prevent disclosure of contents or reconstruction of the document.

For unclassified, unlimited documents, destroy when the report is no longer needed. Do not return it to the originator.

SECURITY CLASSIFICATION OF THIS PAGE (When Data Entered)

REPORT DOCUMENTATION PAGE

READ INSTRUCTIONS BEFORE COMPLETING FORM

1. REPORT NUMBER: ARCCB-TR-88011	2. GOVT ACCESSION NO.
3. RECIPIENT'S CATALOG NUMBER	
4. TITLE (and Subtitle): ELASTIC, STRENGTH, AND STRESS RELAXATION PROPERTIES OF A723 STEEL AND 38644 TITANIUM FOR PRESSURE VESSEL APPLICATIONS	
5. TYPE OF REPORT & PERIOD COVERED: Final	
6. PERFORMING ORG. REPORT NUMBER	
7. AUTHOR(s): J. H. Underwood, R. R. Fujczak, and R. G. Hasenbein	
8. CONTRACT OR GRANT NUMBER(s)	
9. PERFORMING ORGANIZATION NAME AND ADDRESS: US Army ARDEC, Benet Laboratories, SMCAR-CCB-TL, Watervliet, NY 12189-4050	
10. PROGRAM ELEMENT, PROJECT, TASK AREA & WORK UNIT NUMBERS: AMCMS No. 6940.00.6570.012, PRON No. 1A62ZH7QNMSC	
11. CONTROLLING OFFICE NAME AND ADDRESS: US Army ARDEC, Close Combat Armaments Center, Picatinny Arsenal, NJ 07806-5000	
12. REPORT DATE: March 1988	
13. NUMBER OF PAGES: 28	
14. MONITORING AGENCY NAME & ADDRESS (if different from Controlling Office)	
15. SECURITY CLASS. (of this report): UNCLASSIFIED	
15a. DECLASSIFICATION/DOWNGRADING SCHEDULE	

16. DISTRIBUTION STATEMENT (of this Report)

Approved for public release; distribution unlimited.

17. DISTRIBUTION STATEMENT (of the abstract entered in Block 20, if different from Report)

18. SUPPLEMENTARY NOTES

Presented at the Army Symposium on Solid Mechanics, U.S. Military Academy, West Point, NY, 7-9 October 1986.
Published in Proceedings of the Symposium.

19. KEY WORDS (Continue on reverse side if necessary and identify by block number)

Tensile Strength; Lightweight. AW
Elevated Temperature
Stress Relaxation
High Strength Steel
Titanium Alloy
Elastic Properties

20. ABSTRACT (Continue on reverse side if necessary and identify by block number)

Mechanical properties of a high strength steel and a titanium alloy have been measured for application to compound cylinders of steel and titanium subjected to elevated temperature. Results are presented from tests and analyses of elastic and failure strength, stress relaxation, fracture toughness, and microstructure and microhardness. Conclusions are drawn regarding the suitability of the two materials when subjected to conditions typical of cannon fabrication processes and service loading. Keywords:

DD FORM 1 JAN 73 1473 EDITION OF 1 NOV 65 IS OBSOLETE

UNCLASSIFIED

SECURITY CLASSIFICATION OF THIS PAGE (When Data Entered)

TABLE OF CONTENTS

TABLES

LIST OF ILLUSTRATIONS

INTRODUCTION

High strength steel cylinders used for cannon have traditionally been designed primarily to withstand low cycle fatigue loading at high pressure (ref 1). Until recently, elevated temperature exposure or weight limitations have been less important. However, changing service conditions for cannon now often include temperatures well above ambient due to high firing rates. Requirements for air transportation of cannon are more common, so weight has become important. These and other changes have led to the concepts of lightweight materials and compound cylinders for cannon. The work described here is a base technology effort in support of these concepts. Mechanical properties of a high strength steel and a high strength titanium alloy have been measured. Emphasis has been placed on the tests and conditions of interest for a compound cylinder of steel and titanium subjected to a moderately elevated temperature, up to about 400°C.

An initial example can be used to demonstrate some of the technical concerns which arise when a compound cylinder is subjected to elevated temperature. Table I and Figure 1 show the conditions and some results, respectively, of an analysis of steady-state heat flow from the inner diameter (ID) surface to the outer diameter (OD) surface of example cylinders. Three types are shown: a simple cylinder with steel properties; a compound cylinder of steel and titanium; a compound cylinder with a small air gap between steel and titanium. The analysis used the following steady-state equation (ref 2):

---

[1]J. H. Underwood and D. P. Kendall, "Fracture Analysis of Thick-Wall Cylinder Pressure Vessels," Theoretical and Applied Fracture Mechanics, Vol. 2, 1984, pp. 47-58.

[2]F. Kreith, Principles of Heat Transfer, International Textbook Company, Scranton, PA, 1958, pp. 35-38.

$$q = \frac{2\pi k(T_i - T_{i+1})}{\ln(r_{i+1}/r_i)} \qquad (1)$$

in which q is the heat flow per unit length of the cylinder, k is the thermal conductivity of the cylinder material, T_i and r_i are the temperature and radius of the inner surface, and T_{i+1} and r_{i+1} are the temperature and radius of the outer surface. The values of k used for steel and titanium are 9.0 and 1.8 cal/sec-m-°C (ref 3), respectively, obtained from data for two similar alloys, 4340 steel and 6-4 titanium. The k value used for air is 0.0072 cal/sec-m-°C (ref 4).

TABLE I. CONDITIONS FOR ANALYSIS OF SIMPLE AND COMPOUND CYLINDERS

Simple		Compound; Ideal Contact		Compound; Air Gap	
Size	Material	Size	Material	Size	Material
ID: r_1=50 mm OD: r_2=70 mm	steel	ID: r_1=50 mm r_2=60 mm OD: r_3=70 mm	steel titanium	ID: r_1=50 mm r_2=60 mm r_3=60.03 mm OD: r_4=70 mm	steel air titanium

The basic assumptions of the example are that steady-state conduction is the only significant heat transfer through the cylinder wall and that the OD surface is somehow held at a constant temperature of 100°C. A constant OD temperature could, in principle, be accomplished by convection. Equation (1) was first used to calculate a heat flow of 8400 cal/sec-m, associated with an arbitrarily selected ID surface temperature of 150°C for the simple steel

---

[3] Aerospace Structural Metals Handbook, Mechanical Properties Data Center, Traverse City, MI, 1971, Secs. 1206-2; 3707-9.
[4] F. Kreith, Principles of Heat Transfer, International Textbook Company, Scranton, PA, 1958, p. 535.

cylinder. Then this heat flow, which could in principle represent a given cannon firing rate, was used to calculate temperature distributions for the compound cylinders. These results, using Eq. (1), are shown in Figure 1. Note that the low conductivity of the outer section of the compound cylinder causes a significant increase in the ID and mid-wall temperatures, even though ideal thermal contact between sections was assumed. For an air gap of 0.15 percent of the total wall thickness, the inner section is subject to a further significant increase in temperature. In an actual compound cylinder, an effective gap could be present due to the roughness of the contact surfaces, or a gap could develop during fabrication or service due to a mismatch of mechanical or thermal properties of the inner and outer sections.

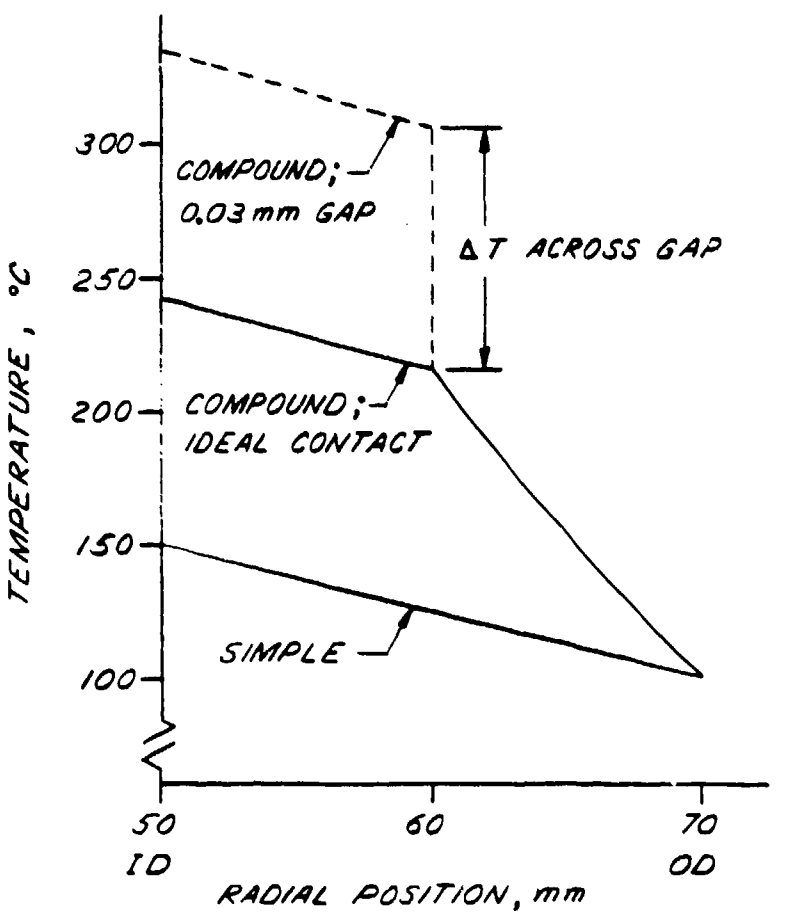

Figure 1. Temperature distribution in simple and compound cylinders; steady-state analysis.

The results from this example show that a compound cylinder of steel and titanium will be considerably more affected by elevated temperature than will a simple steel cylinder. In the following sections the mechanical property tests which were selected to address this concern will be described, and test results will be discussed. These results will be used to answer some questions related to this type of pressure vessel application.

MATERIALS AND TESTS

The alloy steel was purchased as remelt-process forging preforms with the following nominal chemical composition in weight percent: 2.6 Ni, 1.0 Cr, 0.5 Mo, 0.6 Mn, 0.34 C, 0.10 V, 0.008 max P, 0.004 max S. It was rotary forged and heat treated to a nominal yield strength of 1090 MPa. It conforms to ASTM Standard A723, Grade 2 (ref 5).

The titanium alloy was purchased as remelt-process extrusions with nominal yield strength of 1100 MPa. It is commonly referred to as 38644 titanium and has a nominal chemical composition in weight percent of 3.0 Al, 8.0 V, 6.0 Cr, 4.0 Mo, 4.0 Zr.

A schematic summary of the tests is shown in Figure 2 and some of the key test conditions are listed in Table II. The three general categories of tests are strength, stress relaxation, and fracture toughness. Since both test materials were wrought, test specimen orientation was an issue. The orientations of the various tests are sketched in Figure 2, as are the orientations of microstructural investigations which were performed for rationalization of some of the test results.

---

[5]"Standard Specification for Alloy Steel Forgings for High Strength Pressure Component Applications, ASTM A723," 1984 Annual Book of ASTM Standards, Vol. 01.05, ASTM, Philadelphia, PA, 1984, pp. 808-814.

TABLE II. CONDITIONS FOR CHARACTERIZATION TESTS OF STEEL AND TITANIUM CYLINDER MATERIAL

Test	Material	Orientation		Thickness	Width	Length	Temperature °C
Tensile	Steel and titanium	L	overall:	5.1	50.8	184	-54 to +427°
			gage section:	5.1	12.7	64	
	Steel and titanium	C	overall:	5.1	12.7	64	-54 to +204°
			gage section:	5.1	6.4	15	
Stress Relaxation	Steel and titanium	L		5.1	22.2	152	+371 to +482°
	Steel	C		5.1	22.2	152	+371 to +482°
	Titanium	C		2.6	12.7	64	+371 to +482°
Fracture Toughness	Steel	C-R		B=51	W=56	-	+21°
	Titanium	C-R		B=25	W=29	S=116	-54°; +21°

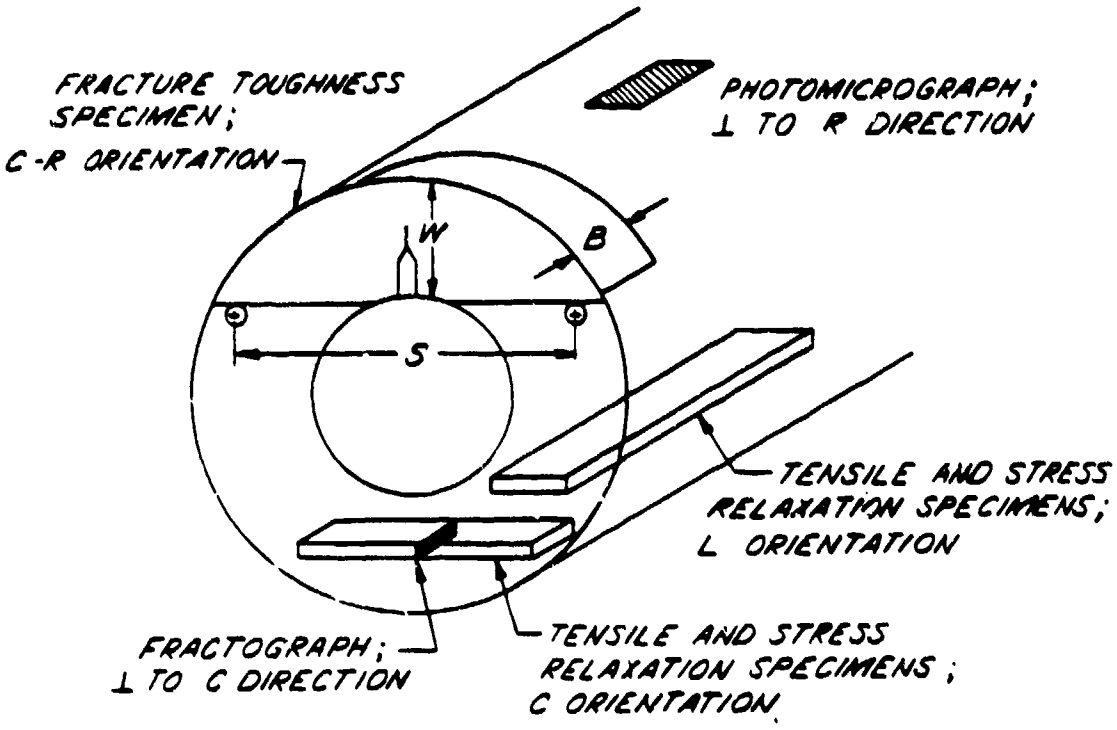

Figure 2. Test orientations in relation to cylindrical geometry.

Tension Tests

Tension-loaded components were used to obtain a variety of strength and deformation data, both elastic and up to failure. The test specimens and procedures were generally similar to those in ASTM Method E-8 (ref 6) and Method E-132 (ref 7). However, it was not possible to follow all recommendations of these methods due to the elevated temperature of many tests. Table II lists both the overall dimensions and those of the gage section for the tension specimens. A combination of resistance strain gages and ambient and elevated temperature extensometers were applied to the specimens to obtain elastic modulus,

---

[6]"Standard Methods of Tension Testing of Metallic Materials, ASTM E-8," 1985 Annual Book of ASTM Standards, Vol. 03.01, ASTM, Philadelphia, PA, 1985, pp. 130-151.

[7]"Standard Test Method for Poisson's Ratio at Room Temperature, ASTM E-132," 1985 Annual Book of ASTM Standards, Vol. 03.01, ASTM, Philadelphia, PA, 1985, pp. 307-309.

Poisson's ratio, yield strength, ultimate strength, and reduction-in-area. Scanning electron fractographs, optical micrographs, and microhardness measurements were obtained for a few selected tension test conditions, as will be discussed in the upcoming Discussion of Results section of this report.

Stress Relaxation Tests

Coupon specimens of the type and orientation shown in Table II and Figure 2 were used to perform stress relaxation tests using the mandrel method described in ASTM Method E-328 (ref 8). This type of test, less common than others used in this work, is summarized in Figure 3. A coupon specimen is clamped over a mandrel of known radius of curvature, R_m. Then, knowing the elastic modulus of the material, the elastic stress at the outer fiber location of the coupon of thickness, h, can be calculated from

$$\sigma_{\text{at load}} = E\left[\frac{h/2}{R_m + h/2}\right] \tag{2}$$

in which the bracketed term is a strain value which is a function of the ratio of specimen thickness to radius-of-curvature. The mandrel, with the specimen clamped in place, is subjected to the desired combination of time and temperature, and as a result some elastic stress may relax. As shown in Figure 3(b), after exposure the permanent specimen deflection, as determined by its concave radius, R_i, is a simple yet quantitative measure of the amount of stress relaxed from the specimen

$$\sigma_{\text{relaxed}} = E\left[\frac{h/2}{R_i + h/2}\right] \tag{3}$$

---

[8]"Standard Recommended Practices for Stress-Relaxation Tests for Materials and Structures, ASTM E-328," 1985 Annual Book of ASTM Standards, Vol. 03.01, ASTM, Philadelphia, PA, 1985, pp. 476-503.

An efficient method for measuring the concave radius of the specimen, R_i, was adapted from the work of Fox (ref 9) and is sketched in Figure 3(c). A gage block in two-point contact with the concave surface establishes a chord of length, S, and a sagitta, Δ, which we found could be easily and accurately measured using a machinist's microscope. Using Euclidean geometry, the radius of curvature can be calculated as

$$R_i = S^2/8\Delta + \Delta/2 \qquad (4)$$

Then, Eq. (4) combined with Eq. (5) can be used to determine the stress relaxed from the outer fiber locations of the coupon specimen as a result of elevated temperature exposure.

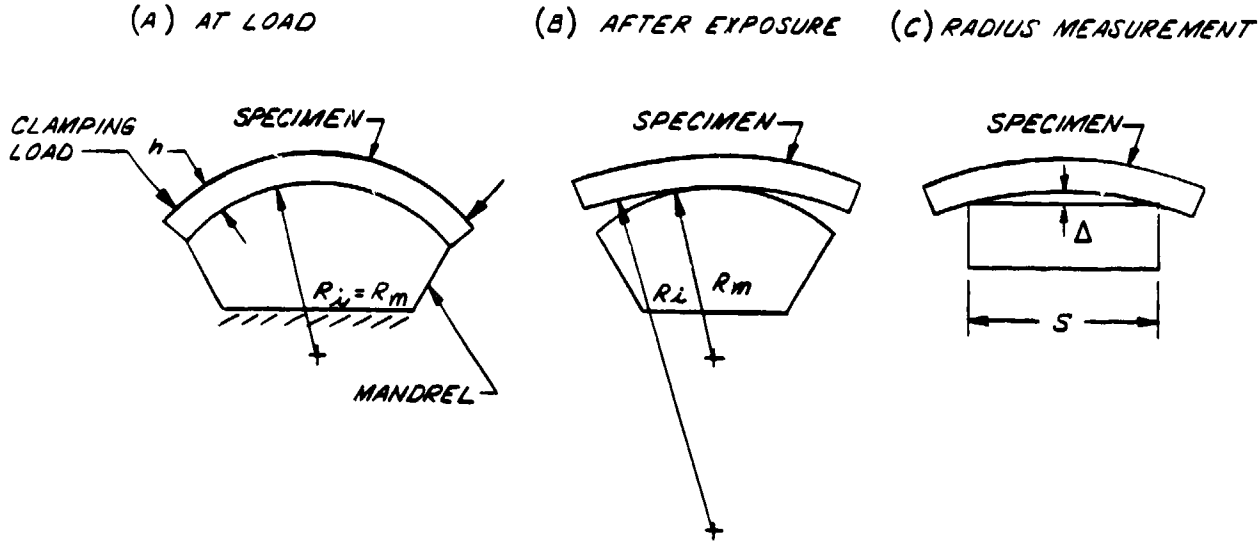

Figure 3. Stress relaxation testing using a strip specimen and mandrel.

---

[9]A. Fox, "A Simple Test for Evaluating Stress Relaxation in Bending," Materials Research and Standards, September 1964, pp. 480-481.

Fracture Toughness Tests

Three-point bend specimens of a recently proposed arc-shaped chord-supported geometry (ref 10) were used to measure the plane-strain fracture toughness, K_{Ic}, of the titanium, see Figure 2. This specimen is not presently included in ASTM Method E-399 (ref 11), but its use is very similar to that of the standard rectangular bend, so the data presented here is believed to be quite correct. The size of the specimens was more than adequate to meet the minimum specimen size requirement of K_{Ic} tests. The C-R orientation, shown in Figure 2, is a common concern in pressure vessels. The crack is in the plane normal to the circumferential direction, which is commonly the direction of the highest tension stress, and the crack grows in the radial direction.

The K_{Ic} tests of the steel used C-R orientation arc-tension specimens of the type described in Method E-399. However, as is often true for cannon steels, the minimum size requirement of Method E-399 could not be met, even though the full wall thickness of the cylinder was used for the specimens. Therefore, the results should be considered to be only an estimate of K_{Ic}. This is mitigated somewhat by the fact that the same factor which precludes a valid K_{Ic} test of the material also tends to prevent rapid elastic-stress-controlled fracture of the cylinder in service. This key factor is the relatively large size of the crack-tip plastic zone relative to the wall thickness of the cylinder.

---

[10] J. H. Underwood, J. A. Kapp, and M. D. Witherell, "Fracture Testing With Arc Bend Specimens," Fracture Mechanics: Seventeenth Volume, ASTM STP 905, (J. H. Underwood, et al., eds.), ASTM, Philadelphia, PA, 1986, pp. 279-296.

[11] "Standard Test Method for Plane-Strain Fracture Toughness of Metallic Materials, ASTM E-399," 1985 Annual Book of ASTM Standards, Vol. 03.01, ASTM, Philadelphia, PA, 1985, pp. 547-582.

DISCUSSION OF RESULTS

Elastic Properties

Figures 4 and 5 summarize the effects of test temperature on two key elastic properties of the steel and titanium. The test specimens were held at the various temperatures for 10-20 minutes before data was recorded, with longer times for the higher temperatures. Figure 4 shows elastic modulus data over a test temperature range of -54° to 427°C, and for two orientations as sketched in Figure 2. The data up to 204°C were obtained from specimens instrumented with resistance strain gages and lead wires which were specially prepared to resist exposure to temperature. The data at higher temperatures were obtained with a high temperature extensometer. For the steel data, a single, visual-best-fit line was drawn through the data for circumferential (C) and longitudinal (L) orientations. The variations from the line are believed to be due more to scatter than to difference in orientation or other factors. The titanium data for the C orientation show a significantly higher modulus than that for the L orientation. Upcoming microstructural results and discussion may relate to this difference in modulus.

The titanium data, in particular, should be compared with data from the literature. The dashed line in Figure 4 is from results of a 150-mm diameter forging of 38644 titanium with about 1100 MPa yield strength (ref 12). It is clear that the results here compare well with the similar data from other work.

Figure 5 shows the Poisson's ratio data for steel and titanium in the C and L orientations. The higher values for titanium are apparent, and the gradual decrease in Poisson's ratio with an increase in temperature can be seen

---

[12] Aerospace Structural Metals Handbook, Battelle Columbus Laboratories, Columbus, OH, 1984, Sec. 3723-1-16.

for both materials, in spite of the scatter. Because of the considerable scatter, linear regression was used to establish a central line through the data for each material. The correlation coefficients were quite low, -0.21 and -0.39, for steel and titanium, respectively. Therefore, the regression line should be used only within the fixed range of data and certainly not for extrapolation. It is believed that the scatter is due to the basic nature of the procedure used to obtain Poisson's ratio. In this procedure, the two sets of strain gage readings and their associated scatter are combined to calculate the result. If there is any significant difference between results for the two orientations, it is obliterated by scatter for both steel and titanium.

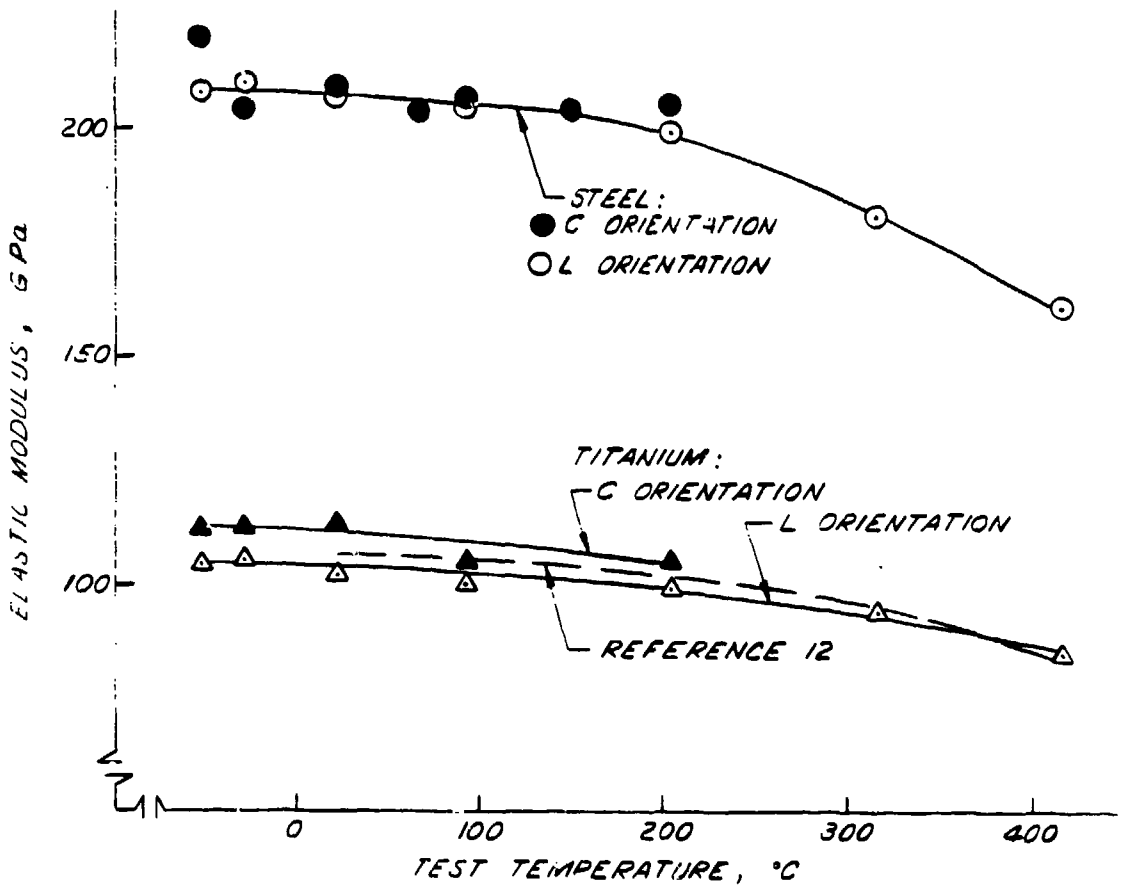

Figure 4. Effect of temperature on elastic modulus for steel and titanium.

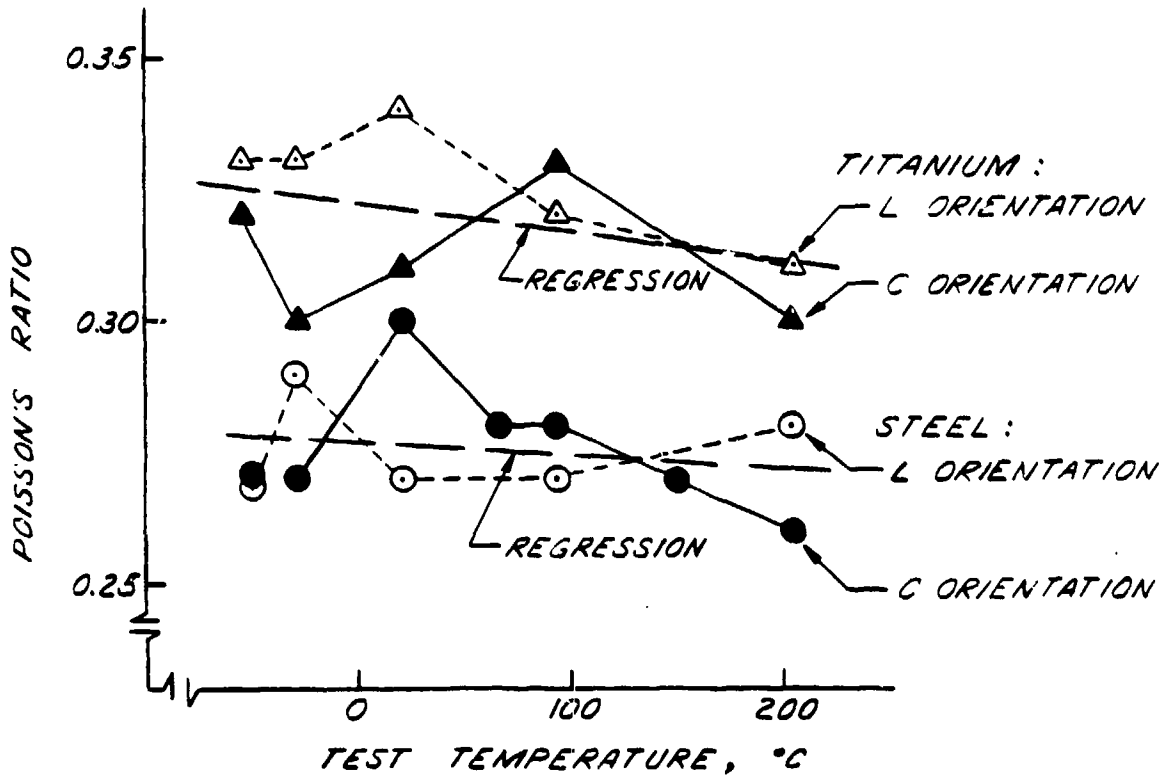

Figure 5. Effect of temperature on Poisson's ratio for steel and titanium.

Mechanical Properties

The mechanical property measurements from tension tests of the steel are shown in Figure 6, including yield and ultimate strengths and reduction-in-area for both C and L orientations. Two replicate tests were performed in all cases. The strength results showed the expected decrease with increasing temperature clearly separate from scatter for all four sets of data. Also as expected, the L orientation specimens were stronger than those of the C orientation.

The reduction-in-area results gave the expected result of a general increase with increasing temperature, but a quite unexpected result of better properties for the C orientation than those for the L orientation. The C orientation is the long transverse direction of the forging which nearly always has poorer reduction-in-area than the L orientation. The opposite result in this

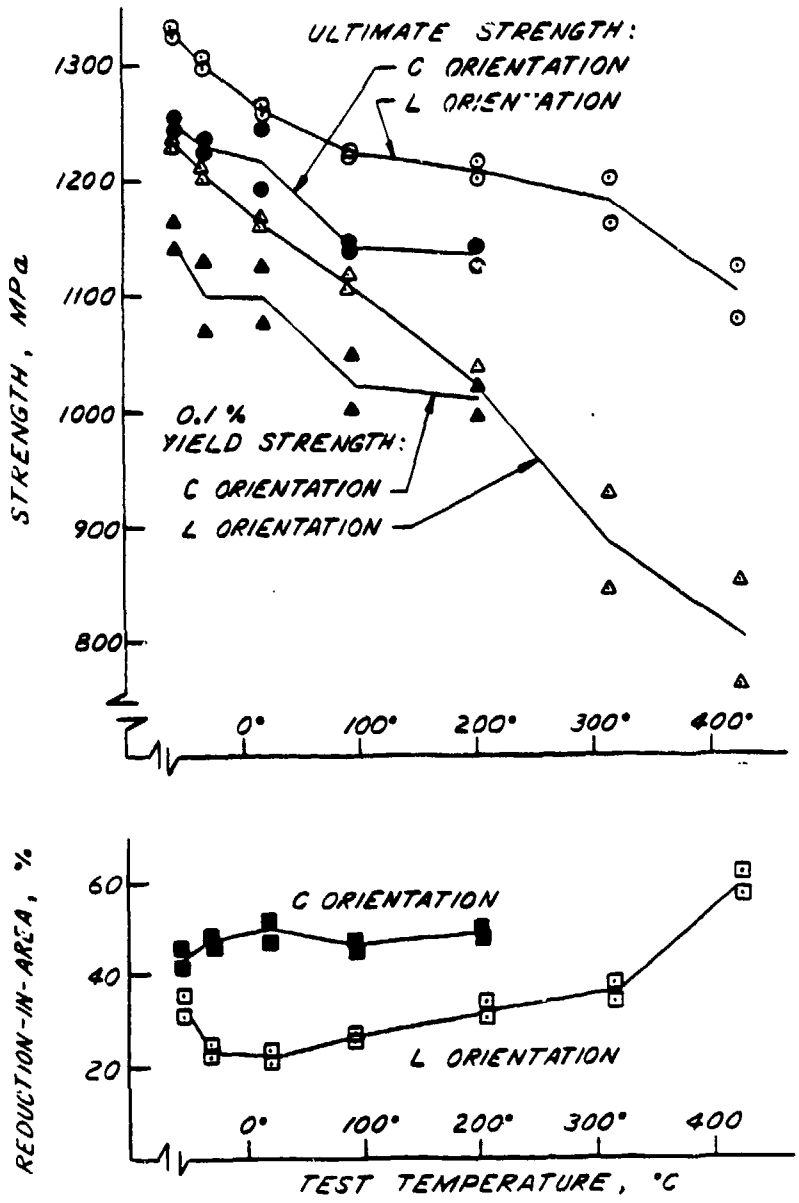

Figure 6. Effect of temperature on tensile mechanical properties of steel.

work is believed to be due to the different geometries of the two specimen orientations. As shown in Table II, the C orientation gage section is nearly square with a width-to-thickness ratio of 1.25, whereas the L orientation gage section is clearly rectangular with a width-to-thickness ratio of 2.50. The larger width, relative to thickness of the L specimen, prevents the unrestrained deformation of the specimen during the final, reduction-in-area portion of the specimen's plastic deformation. This causes a significant depression of the L orientation reduction-in-area. This depression is a reflection of differences in specimen geometry rather than material properties.

The mechanical properties of the titanium are summarized in Figure 7. The strength properties show the expected downward trend with increasing temperature, but unlike the steel results in Figure 6, the L orientation specimens were significantly weaker than the C orientation specimens for both yield and ultimate strength. This is opposite to the usual result for a wrought product, such as this extruded titanium. Consider the longitudinal and transverse ultimate strength results from the literature (ref 12) for a 150-mm diameter 38644 titanium forging shown as dashed and dotted curves, respectively, in Figure 7. The longitudinal direction is stronger, as is usually expected. The reduction-in-area results in Figure 7 for the tests conducted here, show the expected results of better longitudinal properties, although there is some overlap and scatter. However, it is clear that scatter cannot account for the unexpected result in strength measurements for the tests here. This led us to microstructure and microhardness investigations.

---

[12] Aerospace Structural Metals Handbook, Battelle Columbus Laboratories, Columbus, OH, 1984, Sec. 3723-1-16.

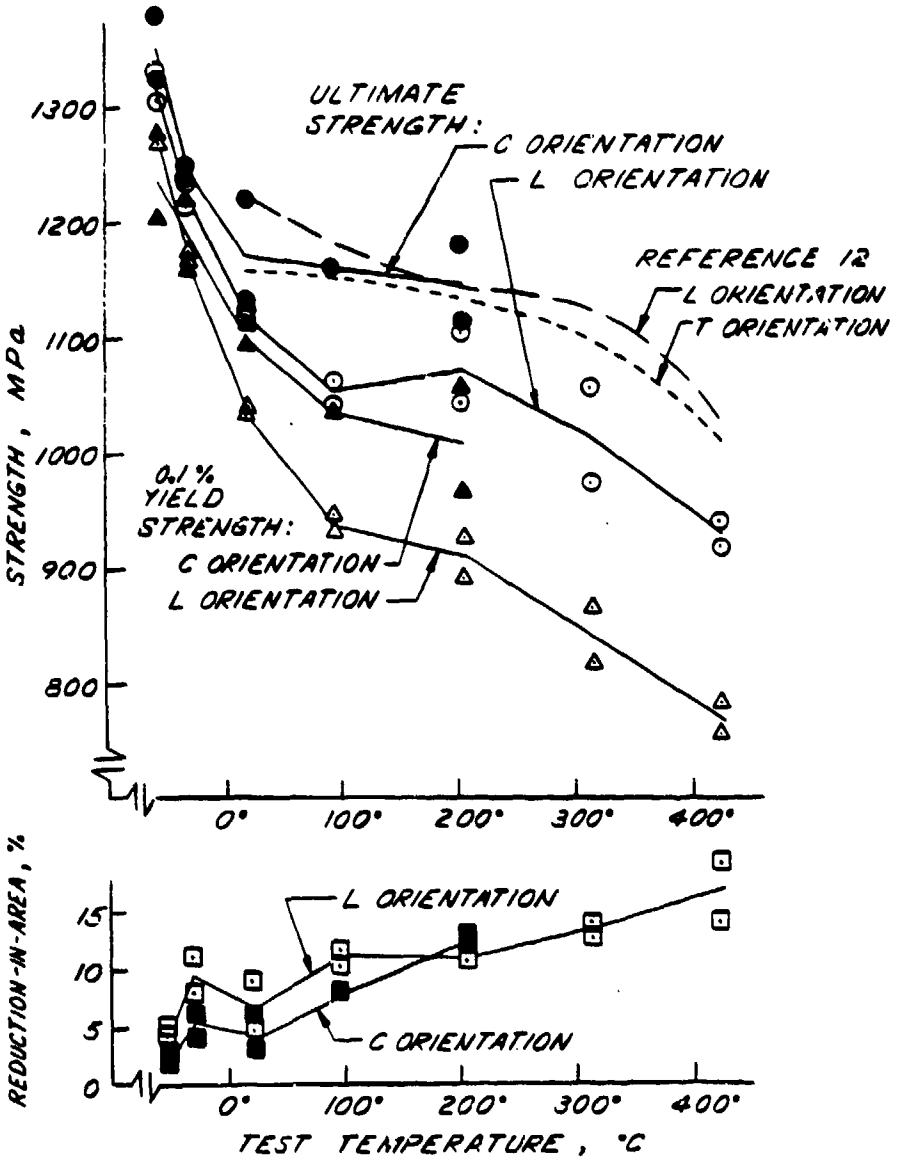

Figure 7. Effect of temperature on tensile mechanical properties of titanium.

Figure 8 shows optical and scanning electron microscope views of the titanium microstructure. Both methods reveal two types of structure, small equiaxed grains and larger grains with considerable elongation in the longitudinal direction. Considering the presence of the elongated grains, the following simple hypothesis was arrived at. If the elongated grains were softer, that would explain the lower longitudinal strength, since the elongated grains would exert significant control on the longitudinal mechanical properties. Five or more replicate Knoop microhardness measurements were made in the gage section of a longitudinal tension specimen which had been loaded to failure. The average results, shown in Table III, show a slightly higher hardness for the elongated grains, so this does not prove the hypothesis. However, measurements from another specimen which had received no loading showed a significantly lower hardness. In addition, when the hardness results were converted to the approximate (ref 13) ultimate strength values shown in Table III, the values corresponded closely to the results of Figure 7. It should be emphasized that the conversion from hardness to ultimate strength is approximate and most appropriate for steels, but it does provide some indication of the strengths of the microstructural constituents of the titanium. The results in Table III indicate that it is the lower undeformed strength of the elongated grains that accounts for the lower strength in the longitudinal orientation of the titanium.

---

[13] Modern Steels and Their Properties, Bethlehem Steel Company, Bethlehem, PA, 1949, p. 221.

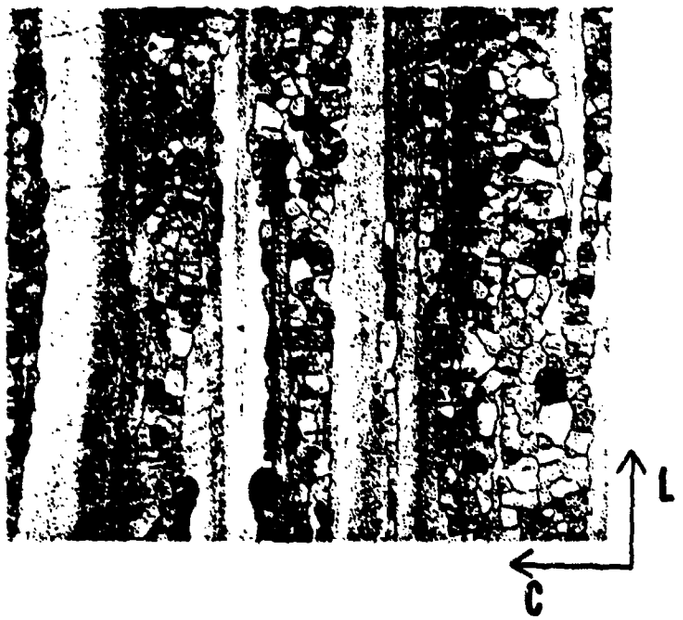

(a) Normal to R orientation.

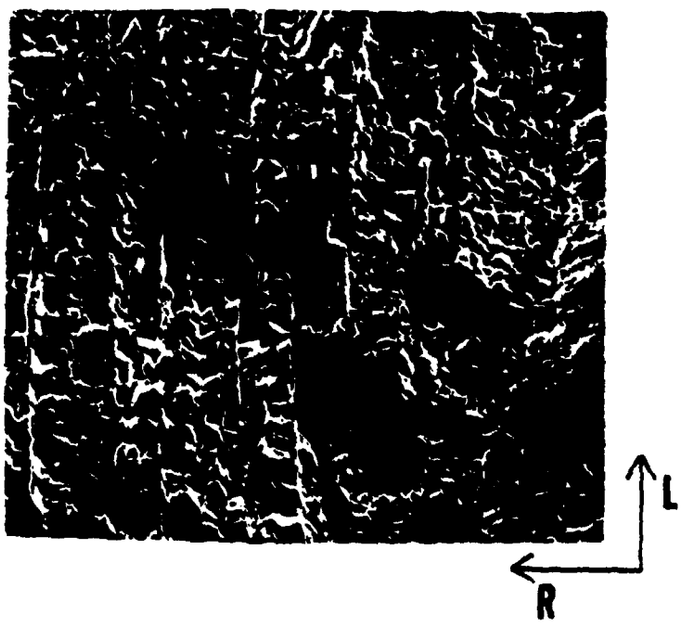

(b) Normal to C orientation.

Figure 8. Optical micrograph and SEM fractograph of titanium (20X).

TABLE III. EFFECT OF TENSILE LOADING ON MICROHARDNESS OF TITANIUM

Large Longitudinal Grains			Small Equiaxed Grains		
Hardness		Approximate	Hardness		Approximate
Mean R_C	Std. Dev. R_C	Ultimate Strength MPa	Mean R_C	Std. Dev. R_C	Ultimate Strength MPa
After Loading:					
38.6	1.3	1240	37.0	0.6	1190
No Loading:					
33.8	1.2	1090	36.8	0.7	1190

Fracture Toughness Results and Analysis

The unusual strength and microstructure results of the foregoing discussion led us to perform fracture toughness tests of the titanium. The results are summarized in Table IV along with typical results for the steel. It is emphasized that the titanium results meet the requirements of the fracture toughness test procedure (ref 11), whereas the steel results cannot meet the requirements because the fracture toughness value is too high for the available specimen size. The average value of fracture toughness for the C-R orientation of the titanium tested here at room temperature, 49 MPa $m^{1/2}$, can be compared with an average literature value (ref 12) of 58 MPa $m^{1/2}$ for the L-T orientation of a 100-mm thick 38644 titanium forging with 1160 MPa yield strength. It is believed that the higher value of toughness from the literature is due to the different test orientation and not to a difference in material quality.

---

[11] "Standard Test Method for Plane-Strain Fracture Toughness of Metallic Materials, ASTM E-399," 1985 Annual Book of ASTM Standards, Vol. 03.01, ASTM, Philadelphia, PA, 1985, pp. 547-582.

[12] Aerospace Structural Metals Handbook, Battelle Columbus Laboratories, Columbus, OH, 1984, Sec. 3723-1-16.

TABLE IV. FRACTURE TOUGHNESS RESULTS FROM STEEL AND TITANIUM

Material	Test Temperature °C	Nominal Yield Strength at 21°C MPa	Fracture Toughness C-R Orientation MPa $m^{\frac{1}{2}}$
Steel	+21°	1090	173, 181
Titanium	+21°	1100	46.6, 51.8
	-54°		40.2, 46.5

The values of measured fracture toughness and yield strength from Table IV can be used to calculate the critical crack size for fast fracture of a cylinder with a crack. Two crack configurations were considered, as shown in Table V.

TABLE V. ANALYSIS OF FAST FRACTURE IN STEEL AND TITANIUM TUBES

Material	Valid Section Size $2.5\ (K_{Ic}/\sigma_y)^2$ mm	Critical Crack Size	
		C-R Orientation a_c mm	C-L Orientation $2C_c$ mm
Steel	66	107.0	91.0
Titanium	5	8.3	6.3

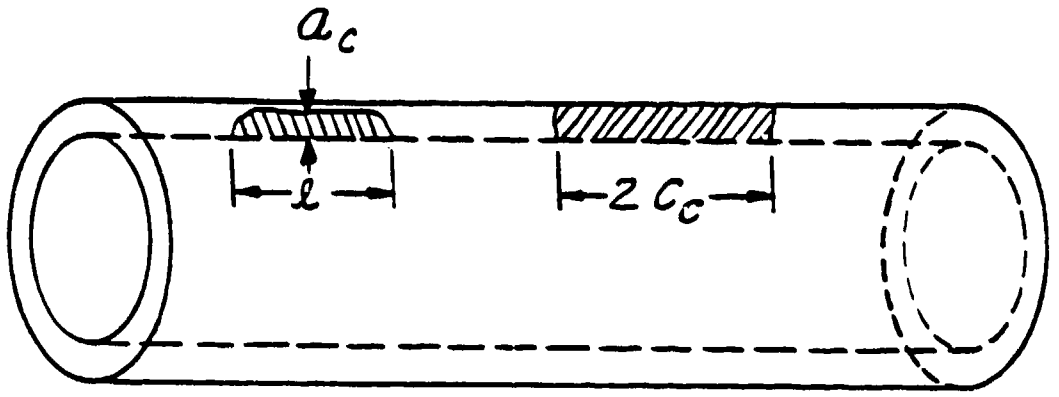

The semi-elliptical-shaped crack from the ID surface of the cylinder is the type which often grows in response to the circumferential direction tensile stress caused by internal pressure. The through-wall crack could be the final result of the ID surface crack, or it could be the result of externally applied damage to the cylinder, such as projectile impact. The through-wall crack would also grow in response to circumferential stress.

An expression which relates the critical value of stress intensity factor for fast fracture, K_{Ic}, to geometry and loading conditions for the ID surface crack is (ref 14)

$$K_{Ic} = 1.12p(\pi a_c)^{1/2} f_s \left[\frac{2(r_2/r_1)^2}{(r_2/r_1)^2 - 1}\right] \quad (5)$$

in which p is the pressure applied to the ID surface of the cylinder and the crack surfaces, a_c is the critical crack size, r_2 and r_1 are the outer and inner radii, and f_s is a geometric factor related to crack depth and shape. An f_s = 0.42 is typical for surface cracks in cylinders (ref 15) for a/1 = 0.2 and $a/(r_2-r_1)$ = 0.5. A related expression for the through-wall crack is (ref 16)

$$K_{Ic} = p(\pi c_c)^{1/2} \left[\frac{r_1}{r_2 - r_1}\right] \quad (6)$$

in which $2c_c$ is the critical crack size.

---

[14] J. H. Underwood, "Stress Intensity Factors for Internally Pressurized Thick-Wall Cylinders," Stress Analysis and Growth of Cracks, ASTM STP 513, ASTM, Philadelphia, PA, 1972, pp. 59-70.

[15] A. P. Parker, J. H. Underwood, J. F. Throop, and C. P. Andrasic, "Stress Intensity and Fatigue Crack Growth in a Pressurized, Autofrettaged Thick Cylinder," Fracture Mechanics: Fourteenth Symposium - Vol. I: Theory and Analysis, ASTM STP 791, (J. C. Lewis and G. Sines, eds.), Philadelphia, PA, ASTM, 1983, pp. I-216-I-237.

[16] J. H. Underwood and J. J. Miller, "Stress Corrosion Cracking of A723 Steel Pressure Vessels: Two Case Studies," High Pressure Technology - Design, Analysis, and Safety of High Pressure Equipment, (D. P. Kendall, ed.), ASME, New York, 1986, pp. 81-90.

Equations (5) and (6) were used to calculate a_c and $2c_c$ using the K_{Ic} values in Table IV. The value of p, 550 MPa, was arbitrarily selected as about one-half of the yield strength of the materials. The values of r_2 and r_1, 60 and 50 mm, respectively, were from one of the geometries considered in Figure 1. The results of the calculations, shown in Table V, vividly demonstrate that the titanium is by far the more fracture-critical material. The initial crack sizes in titanium are less than one-tenth of those in steel. In addition to this drastic difference, a valid section size calculation, shown in Table V, also indicates that the titanium is more fracture-critical. The calculation is patterned after the valid section size requirement of ASTM Method E-399 (ref 11), which gives the section size above which a primarily elastic-stress-controlled, K_{Ic}-type fracture will occur, and below which the crack-tip plastic deformation may prevent a K_{Ic}-type fracture. For the section size of this example, 10 mm, it can be seen that a fast K_{Ic}-type fracture could occur with titanium and could not occur with steel.

Stress Relaxation Results

Twenty-four stress relaxation tests were performed with an initial applied elastic stress of 690 MPa at the outer fiber of the coupon specimen and a two-hour exposure to temperatures from 371°C to 482°C. The results are summarized in Figure 9. The expected trend of increasing stress relaxation with increasing temperature can be seen, and it is clear that titanium is more affected by temperature. Some apparent differences due to orientation can be seen, but

---

[11] "Standard Test Method for Plane-Strain Fracture Toughness of Metallic Materials, ASTM E-399," 1985 Annual Book of ASTM Standards, Vol. 03.01, ASTM, Philadelphia, PA, 1985, pp. 547-582.

considering the data scatter and the fact that the L and C specimens are different in size, no significant orientation effect should be claimed for either material.

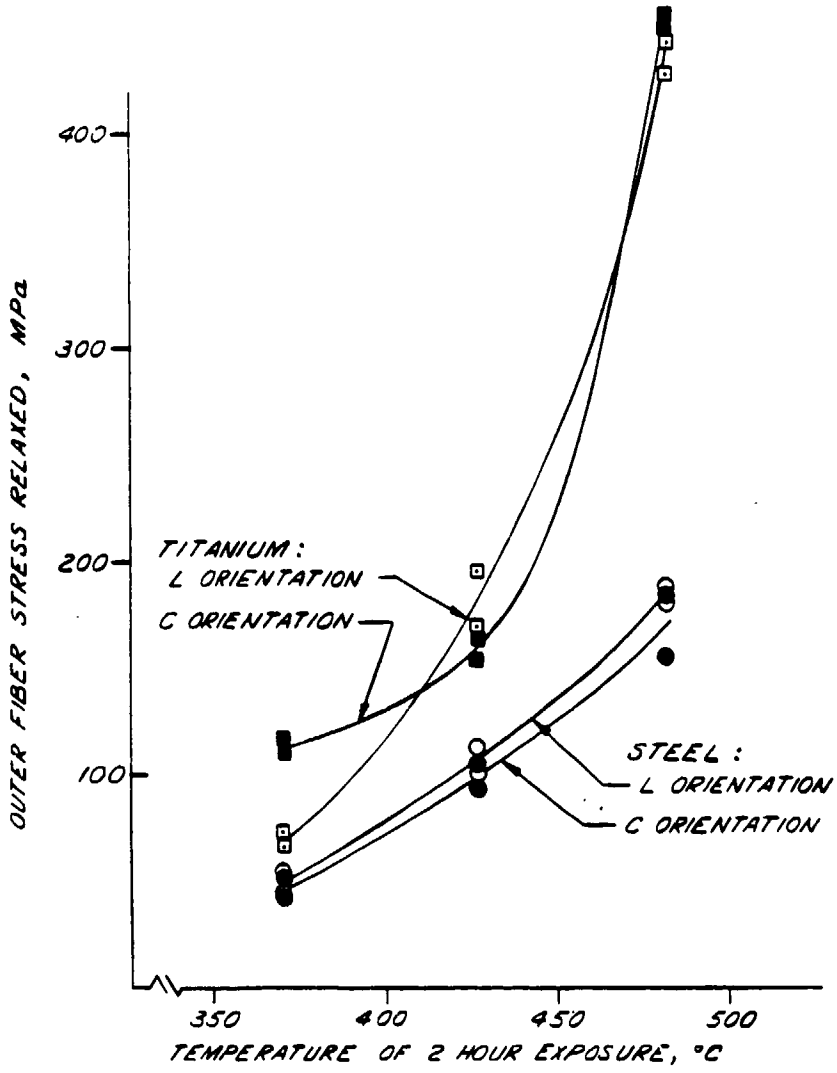

Figure 9. Effect of exposure temperature on amount of stress relaxed from steel and titanium specimens loaded to 690 MPa initial elastic outer-fiber stress.

Two sets of additional tests were performed to investigate the effects on stress relaxation in titanium of (1) longer exposure times, and (2) longer initial elastic stress. Neither of these modifications in test conditions changed the basic nature of the results, but some differences were noted. With regard to exposure time, the average result (from Figure 9) for the two-hour exposure at 371°C for L orientation of the titanium was 69 MPa stress relaxation. The corresponding value for a six-hour exposure was 99 MPa relaxed. With regard to initial stress, the average result (from Figure 9) for the 690 MPa initial stress at 482°C for the T orientation of the titanium was 454 MPa stress relaxation. The corresponding value for a 345 MPa initial stress was 262 MPa relaxed.

One result, the additional stress relaxation for a longer exposure time, was expected. The other result, a higher percentage of the initial stress being relaxed for a lower value of initial stress, was unexpected and should be carefully noted.

SUMMARY AND CONCLUSIONS

The key results and conclusions of this work can be summarized as follows:

Steady-state heat flow analysis of a hypothetical, steel liner-titanium jacket cylinder shows that locations near the ID surface are subjected to significantly higher temperatures than those of an all-steel cylinder with the same overall dimensions and amount of heat flow. The ID temperatures are increased further by the presence of a gap between the liner and the jacket.

A decrease in the elastic modulus with increasing test temperature was noted for both materials in agreement with results from the literature. A slight decrease in Poisson's ratio with increasing temperature was calculated for both materials by linear regression of the somewhat variable results.

The general trend of mechanical properties with increasing temperature was decreasing yield and ultimate strength and increasing reduction-in-area, as would be expected. Two specific results should be noted. First, a misleading indication of lower longitudinal reduction-in-area for the steel, compared with the circumferential orientation, is believed to be a specimen geometry effect rather than a true material property effect. Second, the longitudinal strength properties of the titanium were found to be significantly lower than those of the circumferential orientation. An explanation for this uncommon behavior was found from microstructure and microhardness information which showed grains elongated in the longitudinal direction with noticeably lower hardness than average properties.

The fracture toughness of the titanium was found to be about 30 percent that of the steel, and the critical crack size for the titanium was calculated to be less than 10 percent that of the steel. It is clear that a carefully considered fracture control plan will be necessary for safe use of the titanium in pressure vessel applications.

The titanium and the steel both showed progressively increasing relaxation of stress with increasing temperature, as would be expected. The temperatures at which 25 percent of the initially applied elastic stress was relaxed are 460°C for the steel and 410°C for the titanium. The lower temperature for a given amount of stress relaxation and the steeper gradient of the stress relaxation versus exposure temperature curve demonstrates that the titanium is less resistant than the steel to relaxation of stress at elevated temperatures.

REFERENCES

1. J. H. Underwood and D. P. Kendall, "Fracture Analysis of Thick-Wall Cylinder Pressure Vessels," Theoretical and Applied Fracture Mechanics, Vol. 2, 1984, pp. 47-58.

2. F. Kreith, Principles of Heat Transfer, International Textbook Company, Scranton, PA, 1958, pp. 35-38.

3. Aerospace Structural Metals Handbook, Mechanical Properties Data Center, Traverse City, MI, 1971, Secs. 1206-2; 3707-9.

4. F. Kreith, Principles of Heat Transfer, International Textbook Company, Scranton, PA, 1958, p. 535.

5. "Standard Specification for Alloy Steel Forgings for High Strength Pressure Component Applications, ASTM A723," 1984 Annual Book of ASTM Standards, Vol. 01.05, ASTM, Philadelphia, PA, 1984, pp. 808-814.

6. "Standard Methods of Tension Testing of Metallic Materials, ASTM E-8," 1985 Annual Book of ASTM Standards, Vol. 03.01, ASTM, Philadelphia, PA, 1985, pp. 130-151.

7. "Standard Test Method for Poisson's Ratio at Room Temperature, ASTM E-132," 1985 Annual Book of ASTM Standards, Vol. 03.01, ASTM, Philadelphia, PA, 1985, pp. 307-309.

8. "Standard Recommended Practices for Stress-Relaxation Tests for Materials and Structures, ASTM E-328," 1985 Annual Book of ASTM Standards, Vol. 03.01, ASTM, Philadelphia, PA, 1985, pp. 476-503.

9. A. Fox, "A Simple Test for Evaluating Stress Relaxation in Bending," Materials Research and Standards, September 1964, pp. 480-481.

10. J. H. Underwood, J. A. Kapp, and M. D. Witherell, "Fracture Testing With Arc Bend Specimens," Fracture Mechanics: Seventeenth Volume, ASTM STP 905, (J. H. Underwood, et al., eds.), ASTM, Philadelphia, PA, 1986, pp. 279-296.

11. "Standard Test Method for Plane-Strain Fracture Toughness of Metallic Materials, ASTM E-399," 1985 Annual Book of ASTM Standards, Vol. 03.01, ASTM, Philadelphia, PA, 1985, pp. 547-582.

12. Aerospace Structural Metals Handbook, Battelle Columbus Laboratories, Columbus, OH, 1984, Sec. 3723-1-16.

13. Modern Steels and Their Properties, Bethlehem Steel Company, Bethlehem, PA, 1949, p. 221.

14. J. H. Underwood, "Stress Intensity Factors for Internally Pressurized Thick-Wall Cylinders," Stress Analysis and Growth of Cracks, ASTM STP 513, ASTM, Philadelphia, PA, 1972, pp. 59-70.

15. A. P. Parker, J. H. Underwood, J. F. Throop, and C. P. Andrasic, "Stress Intensity and Fatigue Crack Growth in a Pressurized, Autofrettaged Thick Cylinder," Fracture Mechanics: Fourteenth Symposium - Vol I: Theory and Analysis, ASTM STP 791, (J. C. Lewis and G. Sines, eds.), ASTM, Philadelphia, PA, 1983, pp. I-216-I-237.

16. J. H. Underwood and J. J. Miller, "Stress Corrosion Cracking of A723 Steel Pressure Vessels: Two Case Studies," High Pressure Technology - Design, Analysis, and Safety of High Pressure Equipment, (D. P. Kendall, ed.), ASME, New York, 1986, pp. 81-90.

TECHNICAL REPORT INTERNAL DISTRIBUTION LIST

	NO. OF COPIES
CHIEF, DEVELOPMENT ENGINEERING BRANCH	
ATTN: SMCAR-CCB-D	1
-DA	1
-DC	1
-DM	1
-DP	1
-DR	1
-DS (SYSTEMS)	1
CHIEF, ENGINEERING SUPPORT BRANCH	
ATTN: SMCAR-CCB-S	1
-SE	1
CHIEF, RESEARCH BRANCH	
ATTN: SMCAR-CCB-R	2
-R (ELLEN FOGARTY)	1
-RA	1
-RM	1
-RP	1
-RT	1
TECHNICAL LIBRARY	5
ATTN: SMCAR-CCB-TL	
TECHNICAL PUBLICATIONS & EDITING UNIT	2
ATTN: SMCAR-CCB-TL	
DIRECTOR, OPERATIONS DIRECTORATE	1
ATTN: SMCWV-OD	
DIRECTOR, PROCUREMENT DIRECTORATE	1
ATTN: SMCWV-PP	
DIRECTOR, PRODUCT ASSURANCE DIRECTORATE	1
ATTN: SMCWV-QA	

NOTE: PLEASE NOTIFY DIRECTOR, BENET LABORATORIES, ATTN: SMCAR-CCB-TL, OF ANY ADDRESS CHANGES.

TECHNICAL REPORT EXTERNAL DISTRIBUTION LIST

	NO. OF COPIES
ASST SEC OF THE ARMY RESEARCH AND DEVELOPMENT ATTN: DEPT FOR SCI AND TECH THE PENTAGON WASHINGTON, D.C. 20310-0103	1
ADMINISTRATOR DEFENSE TECHNICAL INFO CENTER ATTN: DTIC-FDAC CAMERON STATION ALEXANDRIA, VA 22304-6145	12
COMMANDER US ARMY ARDEC ATTN: SMCAR-AEE	1
SMCAR-AES, BLDG. 321	1
SMCAR-AET-O, BLDG. 351N	1
SMCAR-CC	1
SMCAR-CCP-A	1
SMCAR-FSA	1
SMCAR-FSM-E	1
SMCAR-FSS-D, BLDG. 94	1
SMCAR-MSI (STINFO) PICATINNY ARSENAL, NJ 07806-5000	2
DIRECTOR US ARMY BALLISTIC RESEARCH LABORATORY ATTN: SLCBR-DD-T, BLDG. 305 ABERDEEN PROVING GROUND, MD 21005-5066	1
DIRECTOR US ARMY MATERIEL SYSTEMS ANALYSIS ACTV ATTN: AMXSY-MP ABERDEEN PROVING GROUND, MD 21005-5071	1
COMMANDER HQ, AMCCOM ATTN: AMSMC-IMP-L ROCK ISLAND, IL 61299-6000	1
COMMANDER ROCK ISLAND ARSENAL ATTN: SMCRI-ENM ROCK ISLAND, IL 61299-5000	1
DIRECTOR US ARMY INDUSTRIAL BASE ENGR ACTV ATTN: AMXIB-P ROCK ISLAND, IL 61299-7260	1
COMMANDER US ARMY TANK-AUTMV R&D COMMAND ATTN: AMSTA-DDL (TECH LIB) WARREN, MI 48397-5000	1
COMMANDER US MILITARY ACADEMY ATTN: DEPARTMENT OF MECHANICS WEST POINT, NY 10996-1792	1
US ARMY MISSILE COMMAND REDSTONE SCIENTIFIC INFO CTR ATTN: DOCUMENTS SECT, BLDG. 4484 REDSTONE ARSENAL, AL 35898-5241	2
COMMANDER US ARMY FGN SCIENCE AND TECH CTR ATTN: DRXST-SD 220 7TH STREET, N.E. CHARLOTTESVILLE, VA 22901	1
COMMANDER US ARMY LABCOM MATERIALS TECHNOLOGY LAB ATTN: SLCMT-IML (TECH LIB) WATERTOWN, MA 02172-0001	2

NOTE: PLEASE NOTIFY COMMANDER, ARMAMENT RESEARCH, DEVELOPMENT, AND ENGINEERING CENTER, US ARMY AMCCOM, ATTN: BENET LABORATORIES, SMCAR-CCB-TL, WATERVLIET, NY 12189-4050, OF ANY ADDRESS CHANGES.

TECHNICAL REPORT EXTERNAL DISTRIBUTION LIST (CONT'D)

	NO. OF COPIES
COMMANDER US ARMY LABCOM, ISA ATTN: SLCIS-IM-TL 2800 POWDER MILL ROAD ADELPHI, MD 20783-1145	1
COMMANDER US ARMY RESEARCH OFFICE ATTN: CHIEF, IPO P.O. BOX 12211 RESEARCH TRIANGLE PARK, NC 27709-2211	1
DIRECTOR US NAVAL RESEARCH LAB ATTN: MATERIALS SCI & TECH DIVISION CODE 26-27 (DOC LIB) WASHINGTON, D.C. 20375	1 1
COMMANDER AIR FORCE ARMAMENT LABORATORY ATTN: AFATL/MN EGLIN AFB, FL 32542-5434	1
COMMANDER AIR FORCE ARMAMENT LABORATORY ATTN: AFATL/MNF EGLIN AFB, FL 32542-5434	1
METALS AND CERAMICS INFO CTR BATTELLE COLUMBUS DIVISION 505 KING AVENUE COLUMBUS, OH 43201-2693	1

NOTE: PLEASE NOTIFY COMMANDER, ARMAMENT RESEARCH, DEVELOPMENT, AND ENGINEERING CENTER, US ARMY AMCCOM, ATTN: BENET LABORATORIES, SMCAR-CCB-TL, WATERVLIET, NY 12189-4050, OF ANY ADDRESS CHANGES.